IOPscience iopscience.iop.org

Home Search Collections Journals About Contact us My IOPscience

Measuring the Junction Temperature of GaInP/GaInAs/Ge Multijunction Solar Cells Using Photoluminescence

This content has been downloaded from IOPscience. Please scroll down to see the full text.

2011 Jpn. J. Appl. Phys. 50 092302

(http://iopscience.iop.org/1347-4065/50/9R/092302)

View the table of contents for this issue, or go to the journal homepage for more

Download details:

IP Address: 140.113.38.11
This content was downloaded on 24/04/2014 at 14:58

Please note that terms and conditions apply.

Japanese Journal of Applied Physics **50** (2011) 092302 **REGULAR PAPER**
DOI: 10.1143/JJAP.50.092302

Measuring the Junction Temperature of GaInP/GaInAs/Ge Multijunction Solar Cells Using Photoluminescence

Gia-Wei Shu, Chiun-Hsiang Tung, Shr-Chang Tung, Po-Chen Su, Ji-Lin Shen*, Min-De Yang[1], Chih-Hung Wu[1], Wu-Ching Chou[2], and Cheng-Hao Ko[3]

Department of Physics and Center for Nanotechnology, Chung Yuan Christian University, Chungli 32023, Taiwan
[1]*Institute of Nuclear Energy Research, P. O. Box 3-11, Lungtan 32500, Taiwan*
[2]*Electrophysics Department, National Chiao-Tung University, Hsinchu 30010, Taiwan*
[3]*Graduate Institute of Automation and Control, National Taiwan University of Science and Technology, Taipei 10672, Taiwan*

Received April 11, 2011; accepted June 11, 2011; published online September 20, 2011

The junction temperatures of the three individual subcells of InGaP/InGaAs/Ge solar cells were measured using photoluminescence (PL) with three different excitation lasers. With the illumination of an extra xenon–mercury lamp, the linear relationship between the PL energy and the illumination level is clearly observed and advantageously used for deriving the junction temperature. Using the Varshni relationship between the PL peak energy and the heat-sink temperature allows us to determine the junction temperature in each subcell.
© 2011 The Japan Society of Applied Physics

1. Introduction

Multijunction tandem solar cells are currently attracting considerable attention owing to their very high conversion efficiencies and potential for space applications.[1–6] Recently, conversion efficiencies over 40% have been demonstrated in three-junction InGaP/InGaAs/Ge solar cells.[7] Three-junction solar cells are designed to operate at high sunlight concentrations using concentrating mirrors or lenses. However, when sunlight is concentrated on solar cells, most of the light is converted into thermal energy in the solar cells, increasing the junction temperature in the solar cells. With an increase in junction temperature, the open-circuit voltage of photovoltaic cells decreases, leading to a decrease in conversion efficiency.[8–10] In addition, the junction temperature may be nonuniform owing to the nonuniformity of the irradiance distribution over a solar cell in a concentrator system. The nonuniform temperature distribution in solar cells may also reduce the open-circuit voltage and conversion efficiency.[11] Thus, developing a method for measuring the junction temperature of the three-junction solar cells directly is important, particularly when cells are under real operation conditions.

An approach to obtain the junction temperature of solar cells has been reported recently.[12] To determine the junction temperature from experiments, a one-dimensional model based on energy balance equations was used. The evaluation of junction temperature from this method, however, involves measurements through contacts. Thus, it is desirable to develop a rapid, nondestructive, and noncontact method to characterize the junction temperature of solar cells. Very recently, we have introduced a technique for measuring the junction temperature of GaAs solar cells using photoluminescence (PL).[13] This technique measures the PL under the pulse width modulation of excitation laser. The junction temperature was determined by the calibration of the temperature-dependent PL and/or the fit of the high-energy tail in PL. Using this technique, the nonuniform junction temperature of solar cells can be detected locally because the spot size of the excitation laser beam is small. In this study, we used the PL technique again to determine the junction temperatures of three-junction InGaP/InGaAs/Ge solar cells. The PL within each subcell was measured using various pumping lasers with different excitation energies. An extra light source (xenon–mercury lamp) with various illumination levels was used to increase the junction temperatures of the solar cells. The linear relationship between the junction temperature and the illumination level of the xenon–mercury lamp is used to characterize the individual junction temperature sof all subcells in the three-junction InGaP/InGaAs/Ge solar cells.

2. Experiment Methods

The samples investigated here were composed of cascade-type InGaP/InGaAs/Ge junctions connected in series. The details of the sample structure are described elsewhere.[14] Briefly, the top $In_{0.5}Ga_{0.5}P$, middle $In_{0.01}Ga_{0.99}As$, and bottom Ge subcells were all lattice-matched and grown on a p-type Ge substrate. The InGaP subcell was connected to the InGaAs subcell by a p-AlGaAs/n-InGaP tunnel junction. The InGaAs subcell was connected to the Ge subcell by a p-GaAs/n-GaAs tunnel junction. Before characterization, the current-voltage characteristics of the three-junction InGaP/InGaAs/Ge solar cell were measured to confirm the near-ideal diode behavior. The PL measurements of the top, middle, and bottom junctions were carried out using CW solid-state lasers with wavelengths of 532, 780, and 1064 nm, respectively, as the excitation sources. The PL signal was focused into a 0.75 m monochromator whose output was detected by a photomultiplier (PMT) tube or an extended InGaAs photodetector. The PL signal was measured by a lock-in amplifier in conjunction with a mechanical chopper and recorded by a computer. An additional light source, a 300 W xenon–mercury lamp, was used to produce heat in the three-junction InGaP/InGaAs/Ge solar cell under short-circuit conditions. The light from the xenon–mercury lamp does not contribute to the PL signal since it does not pass through the mechanical chopper. For the temperature-dependent PL measurements, the sample was mounted in a closed-cycle helium cryostat at a temperature between 200 and 300 K.

3. Results and Discussion

Figure 1 shows a plot of the room-temperature PL values of

*E-mail address: jlshen@cycu.edu.tw

 © 2011 The Japan Society of Applied Physics

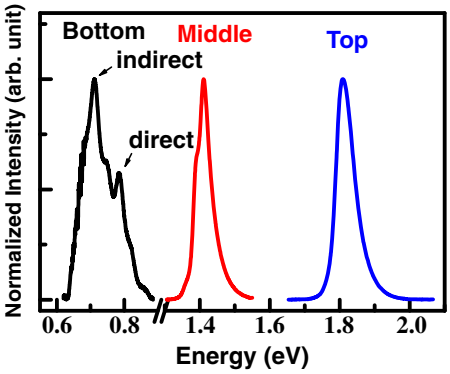

Fig. 1. (Color online) Photoluminescence (PL) spectra of the three-junction InGaP/InGaAs/Ge solar cell obtained using three different excitation lasers. The PL values of the top, middle, and bottom subcells were obtained by lasers with excitation wavelengths of 532, 780, and 1064 nm, respectively. The direct and indirect interband transitions in Ge in the bottom subcell are marked by arrows.

the InGaP top, InGaAs middle, and Ge bottom subcells. The spectra clearly reveal an InGaP signal located at around 1.9 eV and a GaAs signal located at around 1.5 eV, which originated from the top and middle subcells, respectively. In the bottom subcell, two main PL peaks are observed, where the high-energy (low-energy) peak located at 0.8 (0.67) eV is attributed to the direct (indirect) transition in Ge.[15] For consistency, we chose the direct transition (0.8 eV peak) to monitor the junction temperature of the Ge bottom subcell. Figures 2(a)–2(c) display the PL peaks as a function of the illumination level induced by an extra xenon–mercury lamp for the top, middle, and bottom subcells, respectively. As the illumination level increases, the peak energies in all subcells shift toward the low-energy side. This phenomenon is explained by the increase in temperature due to the increased heating by the irradiance. The open circles in Figs. 3(a)–3(c) show the PL peak energies versus the illumination level of the xenon–mercury lamp for the top, middle, and bottom subcells, respectively. It is obvious that there is a linear relationship between the peak energy and the illumination level for each subcell. The solid lines in Fig. 3 show the linear fittings of experimental data, and the slopes are 17.0, 18.9, and 11.3 meV/mW for the top, middle, and bottom subcells, respectively. The linear dependence of PL peak energy on illumination level is advantageously used to determine the junction temperature of the three-junction solar cell.

When the solar cell is irradiated by light, the photo-generated electron-hole pairs generate the voltage due to charge carrier separation and lead to the screening of the built-in electric field in the depletion region. This phenomenon is attributed to the photovoltaic effect, which might cause the shift in PL peak energy. To determine the contribution of the photovoltaic effect to the shift in PL peak energy, the forward-bias dependence of PL measurements was measured (the screening of the built-in electric field is equivalent to the introduction of a forward bias). Figure 4 shows the PL values at three different biases from the three-junction InGaP/InGaAs/Ge solar cell. It is noted that the PL peak energies remain unchanged in all subcells under the forward bias (the applied voltage is increased from

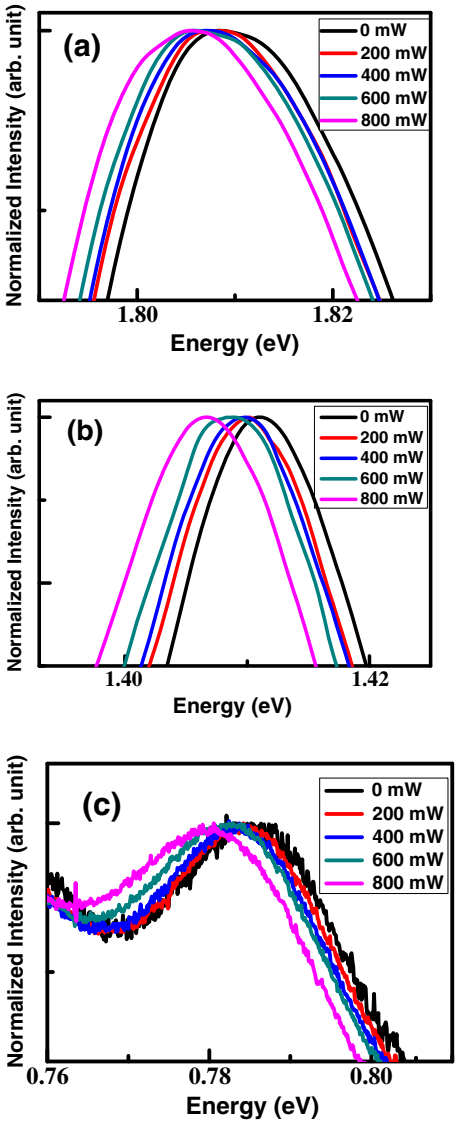

Fig. 2. (Color online) Normalized PL spectra of (a) top InGaP, (b) middle InGaAs, and (c) bottom Ge subcells under different illumination levels of an extra xenon–mercury lamp.

0 to 2.5 V). In fact, the photovoltaic effect should not play an important role in the screening of the built-in electric field since our experimental setup is under the short-circuit conditions. Thus, we conclude that the photovoltaic effect does not contribute to the PL peak shift when the solar cell is under the illumination of the xenon–mercury lamp.

To determine the junction temperature of the three-junction cell, we need to calibrate the effect of heating on the energy change of the PL peak by measuring the dependence of PL on the heat-sink temperature. Figure 5 shows the dependence of the heat-sink temperature on the PL peak energy of the three-junction InGaP/InGaAs/Ge solar cells from 200 to 300 K. The PL peaks red-shift with increasing the heat-sink temperature owing to band gap shrinkage. The energies of the PL peaks in the three-junction InGaP/InGaAs/Ge solar cell as a function of the heat-sink temperature are shown by the open squares in Fig. 6. The redshift of PL peak energy as a function of the temperature can be analyzed according to the Varshni equation[16]

© 2011 The Japan Society of Applied Physics

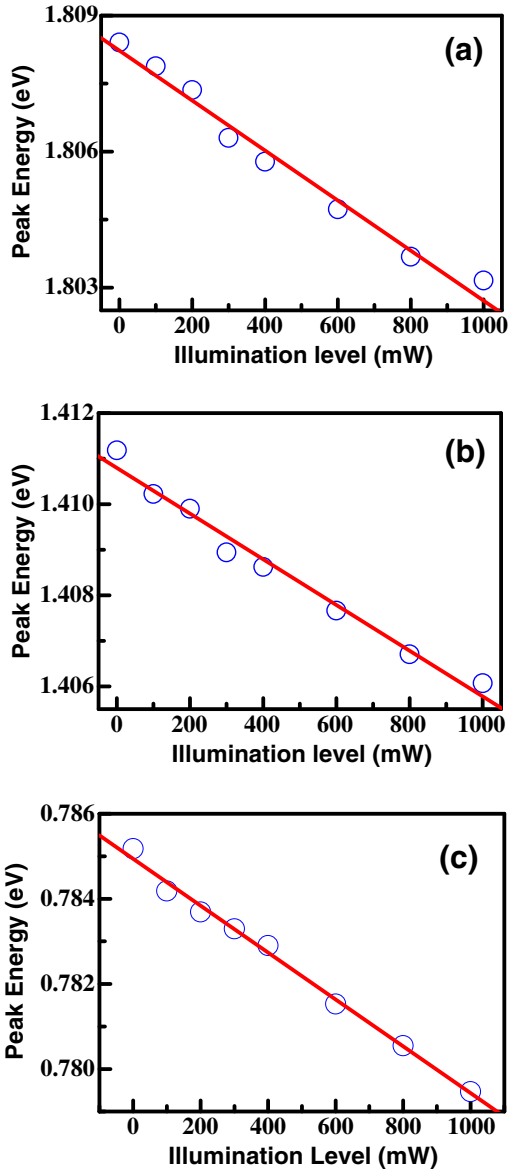

Fig. 3. (Color online) PL peak energies of (a) top InGaP, (b) middle Inga As, and (c) bottom Ge subcells versus the illumination level of the xenon–mercury lamp. The solid lines show the linear fittings of experimental data.

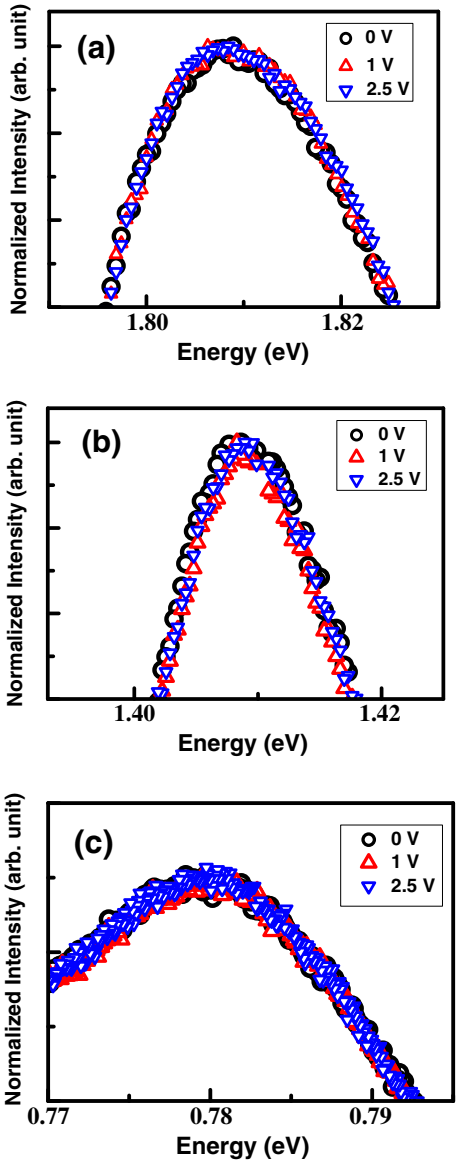

Fig. 4. (Color online) PL spectra at three different voltages from (a) top InGaP, (b) middle InGaAs, and (c) bottom Ge subcells.

$$E_g(T) = E_g(0) - \frac{\alpha T^2}{T + \beta}, \quad (1)$$

where $E_g(0)$ is the energy band gap at 0 K, and α and β are the Varshni parameters. In the high-temperature region, the effect of band gap shrinkage shows linearity with temperature in the Varshni equation.[17] According to eq. (1), the PL peak energy is plotted against the heat-sink temperature, as shown by the solid lines in Fig. 6. From the fits, α (β) values were found to be 0.37, 0.28, and 0.70 meV/K (160, 120, and 360 K) for the InGaP, InGaAs, and Ge, respectively. From the slopes of the solid lines in Fig. 6, the temperature coefficient (dE/dT) of PL was calculated to be 0.30, 0.25, and 0.46 meV/K for the top, middle, and bottom subcells, respectively. These slopes can be used for evaluating the junction temperature with different illumination levels (Fig. 2).

The open circles in Figs. 7(a)–7(c) show the junction temperature versus the illumination level from the top InGaP, middle InGaAs, and bottom Ge subcells, respectively. As can be seen, the junction temperature increases with the illumination level, which induces the redshift of PL peaks. Moreover, the temperature increase measured by this technique is proportional to the illumination level, indicating that the measurement is sensitive to the dissipated optical power. The solid lines in Fig. 7 are linear fits to the experimental data. The power coefficients (dT_j/dP, where T_j is the junction temperature) of the junction temperatures are 1.70×10^{-2}, 1.89×10^{-2}, and 1.13×10^{-2} K/mW for the top, middle, and bottom subcells, respectively. This linear relationship reveals that the effect of the illuminated optical power on the junction temperature of the solar cell is significant and has a sufficient temperature resolution. Also, the linear relationship between the illumination level and the junction temperature is an indication that the PL technique can be used as a convenient tool for measuring the junction temperature of solar cells. It is noted that the temperatures of the subcell are different under the same illumination

© 2011 The Japan Society of Applied Physics

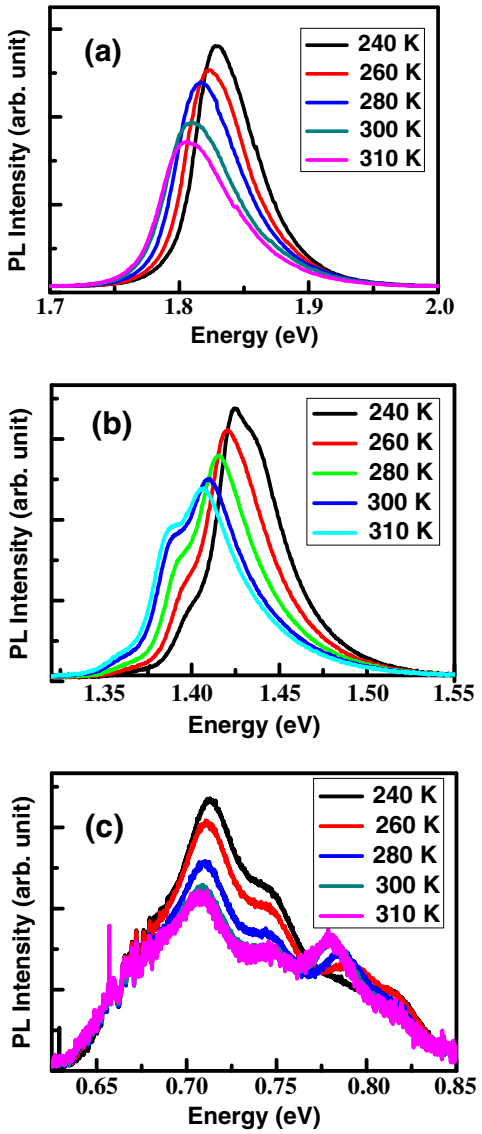

Fig. 5. (Color online) Temperature dependence of the PL spectra for (a) top InGaP, (b) middle InGaAs, and (c) bottom Ge subcells.

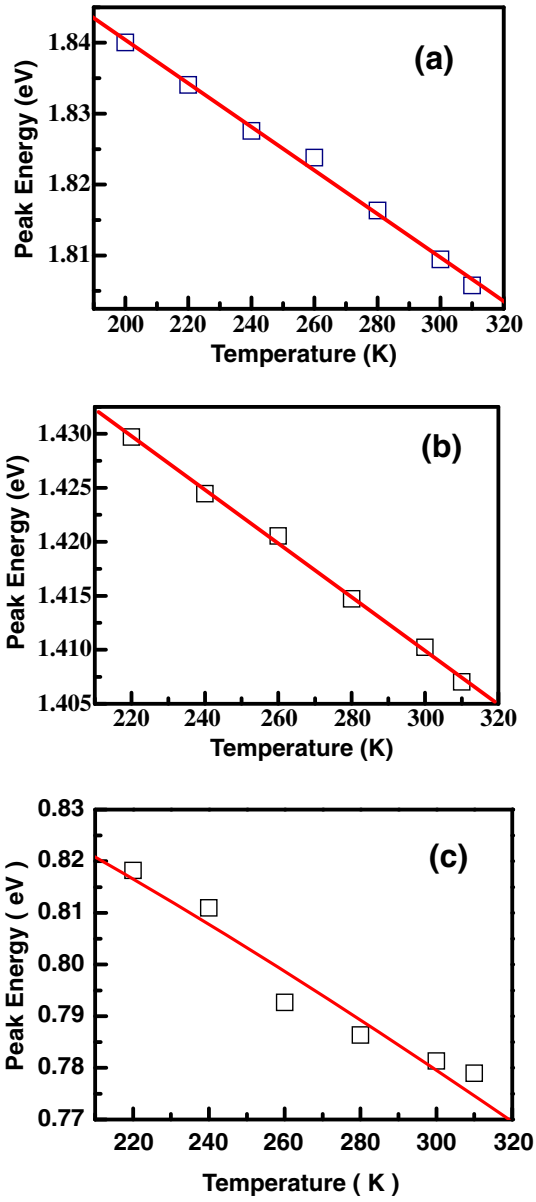

Fig. 6. (Color online) Dependence of PL peak energies on the temperatures of (a) top InGaP subcell, (b) middle InGaAs, and (c) bottom Ge subcells. The lines show the results calculated using eq. (1).

conditions. For example, the junction temperatures under the illumination of the xenon–mercury lamp with 1000 mW are 313, 314, and 307 K for the top, middle, and bottom subcells, respectively. It is obvious that the temperature of the bottom subcell is much lower than that of the top (middle) subcell. A similar phenomenon has been recently observed for GaInP/GaAs/Ge solar cells under concentrated sunlight.[18] The different temperatures of the subcells are attributed to the nonuniform spectral distribution from the xenon–mercury lamp, which generates light with higher output power in the ultraviolet and visible regions, and lower output power in the infrared region. In addition, the different thickness of the base layer as well as the thermal resistance of each subcell may also lead to the different junction temperatures of subcells under the same light source.

To verify the validity of the measured junction temperature using the above method (measuring the energy shift of the PL peak), another approach using the fit of the high-energy slope to the PL spectrum was also investigated. The carrier temperature (T_C) obtained from the high-energy slope in luminescence has been used to obtain the junction temperature of a device recently.[19] Figure 8 shows the high-energy tails of PL in the top InGaP junction with and without the illumination of the xenon–mercury lamp. A change in the high-energy tail of the PL is observed. The high-energy tail of the PL can be analyzed by the function[19]

$$I(\hbar w) \sim \exp\left(-\frac{\hbar w}{kT_C}\right), \tag{2}$$

where T_C reflects the carrier temperature of the thermalized electrons. The carrier temperature of the top InGaP junction versus the illumination level of the xenon–mercury lamp is displayed in the upper-right inset in Fig. 8. The carrier temperatures linearly correlate with the illumination level. For determining the lattice temperature (T_L) from T_C, we calibrated the relationship between T_C and T_L by measuring the dependence of PL on temperature. The lower-left inset in Fig. 8 shows the interrelationship between T_C and T_L for the

© 2011 The Japan Society of Applied Physics

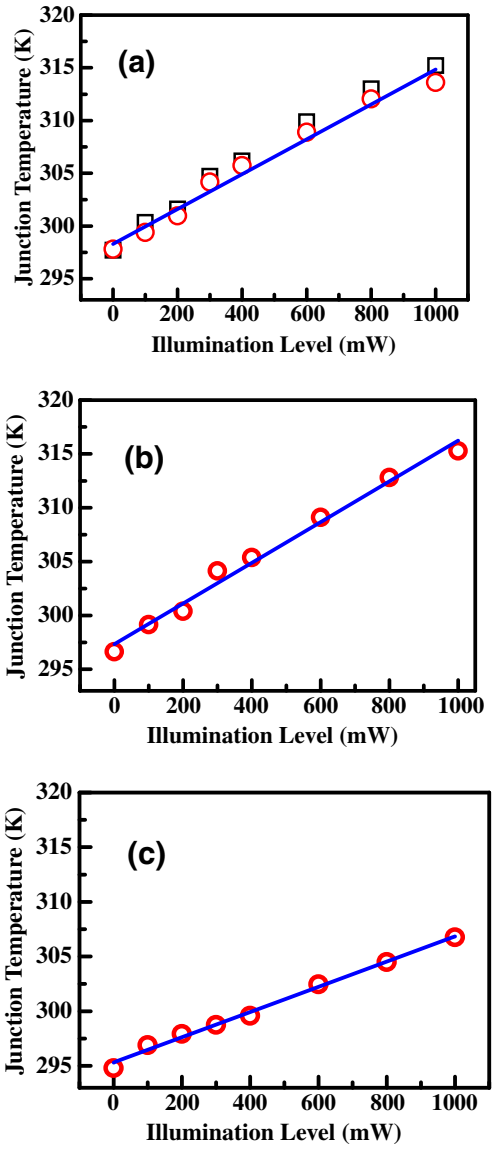

Fig. 7. (Color online) Junction temperature (open circles) versus illumination level of the xenon–mercury lamp from (a) top InGaP, (b) middle InGaAs, and (c) bottom Ge subcells. The solid lines indicate the linear fittings of experimental data. The open squares in (a) show the junction temperatures obtained by fitting the high-energy slope to the PL spectrum.

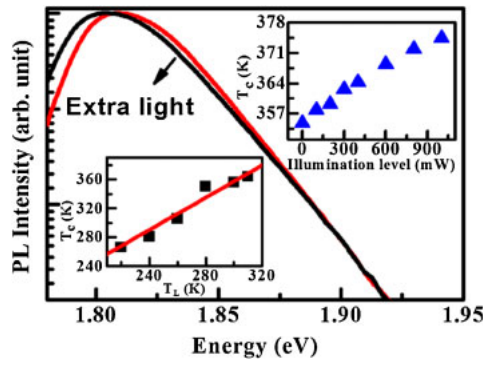

Fig. 8. (Color online) High-energy tails of the PL in the top InGaP junction with and without extra illumination of the xenon–mercury lamp (1000 mW). The upper-right inset shows a plot of the carrier temperature (T_C) versus the illumination level of the xenon–mercury lamp. The lower-left inset shows the carrier temperature as a function of the lattice temperature (T_L). The solid line in the inset is a guide for the eye.

top InGaP junction from 200 to 300 K. The T_C of the junction layer linearly correlates with T_L, as shown by the solid line in the inset. We used this proportionality to estimate the T_L of the InGaP junction, and the obtained values of T_L are shown by the open squares in Fig. 7(a). The good agreement between the two approaches demonstrates the validity of the measured junction temperatures in the multijunction solar cells.

4. Conclusions

The individual junction temperatures of all subcells in three-junction InGaP/InGaAs/Ge solar cells were determined using PL. A linear relationship between the junction temperature and the illumination level of the xenon–mercury lamp was confirmed. The junction temperature of each subcell was determined according to calibration based on the Varshni equation. We also studied the carrier temperature of the top junction layer to confirm the result determined from the peak energy shift in the PL. The method described in this study is rapid, noncontact, and nondestructive, and it can be applied to the evaluation of the individual junction temperatures of three-junction InGaP/InGaAs/Ge solar cells.

Acknowledgements

This project was supported in part by the National Science Council under grant number 97-2112-M-033-004-MY3 and by the Institute of Nuclear Energy Research under grant number 1002001INER042.

1) T. Takamoto, E. Ikeda, H. Kurita, and M. Ohmori: Appl. Phys. Lett. **70** (1997) 381.
2) M. Yamaguchi: Sol. Energy Mater. Sol. Cells **75** (2003) 261.
3) C. G. Zimmermann: J. Appl. Phys. **100** (2006) 023714.
4) O. Korech, B. Hirsch, E. A. Katz, and J. M. Gordon: Appl. Phys. Lett. **91** (2007) 064101.
5) T. Kirchartz, U. Rau, M. Hermle, A. W. Bett, A. Helbig, and J. H. Werner: Appl. Phys. Lett. **92** (2008) 123502.
6) W. Guter, J. Schöne, S. P. Philipps, M. Steiner, G. Siefer, A. Wekkeli, E. Welser, E. Oliva, A. W. Bett, and F. Dimroth: Appl. Phys. Lett. **94** (2009) 223504.
7) R. R. King, D. C. Law, K. M. Edmondson, C. M. Fetzer, G. S. Kinsey, H. Yoon, R. A. Sherif, and N. H. Karam: Appl. Phys. Lett. **90** (2007) 183516.
8) M. Y. Feteha and G. M. Eldallal: Renewable Energy **28** (2003) 1097.
9) D. Meneses-Rodríguez, P. P. Horley, J. González-Hernández, Y. V. Vorobiev, and P. N. Gorley: Sol. Energy **78** (2005) 243.
10) K. Nishioka, T. Takamoto, T. Agui, M. Kaneiwa, Y. Uraoka, and T. Fuyuki: Sol. Energy Mater. Sol. Cells **90** (2006) 57.
11) R. W. Sanderson, D. T. O'Donnell, and C. E. Backus: Proc. 14th IEEE Photovoltaic Specialists Conf., 1980, p. 431.
12) A. Royne, C. J. Dey, and D. R. Mills: Sol. Energy Mater. Sol. Cells **86** (2005) 451.
13) M. D. Yang, W. C. Liao, G. W. Shu, Y. K. Liu, J. L. Shen, C. H. Wu, W. C. Chou, and Y. C. Lee: Solid State Commun. **150** (2010) 1217.
14) M. D. Yang, Y. K. Liu, J. L. Shen, C. H. Wu, C. A. Lin, W. H. Chang, H. H. Wang, H. I. Yeh, W. H. Chan, and W. J. Parak: Opt. Express **16** (2008) 15754.
15) T. H. Cheng, C. Y. Ko, C. Y. Chen, K. L. Peng, G. L. Luo, C. W. Liu, and H. H. Tseng: Appl. Phys. Lett. **96** (2010) 091105.
16) J. C. Zhang, Y. H. Zhu, T. Egawa, S. Sumiya, M. Miyoshi, and M. Tanaka: Appl. Phys. Lett. **92** (2008) 191917.
17) N. C. Chen, Y. N. Wang, C. Y. Tseng, and Y. K. Yang: Appl. Phys. Lett. **89** (2006) 101114.
18) M. Cui, N. Chen, J. Wu, L. Liu, P. Wang, Y. Wang, and Y. Bai: Proc. SPIE **6841** (2007) 684117.
19) P. Manninen and P. Orreveteläinen: Appl. Phys. Lett. **91** (2007) 181121.

© 2011 The Japan Society of Applied Physics